Summer 6-26-2014

Investigation of transpiration cooling with local thermal non-equilibrium model: Effects of different thermal boundary conditions at the porous-fluid interface

Zheng Huang
Tsinghua University

Yin-Hai Zhu
Tsinghua University

Pei-Xue Jiang
Tsinghua University

Yan-Bin Xiong
Beijing institute of Astronautical System Engineering

Proceedings of the 5th International Conference on Porous Media and its Applications in Science and Engineering
ICPM5
June 22-27, 2014, Kona, Hawaii

INVESTIGATION OF TRANSPIRATION COOLING WITH LOCAL THERMAL NON-EQUILIBRIUM MODEL: EFFECTS OF DIFFERENT THERMAL BOUNDARY CONDITIONS AT THE POROUS-FLUID INTERFACE

Zheng Huang， Yin-hai Zhu and Pei-Xue Jiang
Department of Thermal Engineering, Tsinghua University, Beijing 100084, China

Yan-Bin Xiong
Beijing institute of Astronautical System Engineering, Beijing 100076, China

ABSTRACT

In this study, the main stream coupled with a porous medium with local thermal non-equilibrium assumption is analyzed. The flow inside the porous material is modelled using the Darcy–Brinkman–Forchheimer equation and the incompressible Navier-Stokes equations are solved for the main stream. Several couple conditions between the main flow temperature and the temperatures of the solid matrix and coolant flow at the fluid/porous interface is calculated. The results show that the Model C assumes the main flow temperature equals the solid phase temperature and the main flow heat flux is all imposed on the solid phase gives the most reasonable answer.

INTRODUCTION

A transpiration cooling system is usually constructed of a porous structure in which the cooling fluid can flow through the heated surface. And the transpiration cooling is well recognized as a promising means to reduce heat loads on the leading edges and noses of hypersonic vehicles because it forms a coolant film over the surface, and thicken the boundary layer which, therefore, reduces the temperature gradient at the wall. Moreover, there is strong heat transfer between the coolant and the porous structure due to multiple cooling channels and the large heat transfer area within the porous material. Figure 1 shows this cooling principle. The numerical investigations of transpiration cooling can be divided into two categories. The first kind of the analysis model calculates the main flow boundary layer zone and the porous zone separately. The injection of coolant was set as a normal velocity inlet boundary condition and the Navier Stokes equations were simplified in the main flow boundary zone, laminar or turbulence. Then the high temperature main flow was simplified as a heat flux or temperature boundary condition to solve the temperature distribution within the porous zone [1-2]. The second kind of the numerical model coupled the main flow and porous zone which avoid the uncertainty of choosing proper boundary condition for the heat side of the porous zone [3-4]. However, the heat transfer processes within the porous matrix were assumed thermal equilibrium between matrix and flow temperatures in those two categories of models. Due to the low thermal conductivity of ceramic materials commonly used in case of engine transpiration cooling, the thermal non-equilibrium effects will be pronounced. Furthermore, a heat flux boundary condition was applied on the hot wall or the matrix surface temperature equals the flow exit temperature [5] when the local thermal non-equilibrium model was used.

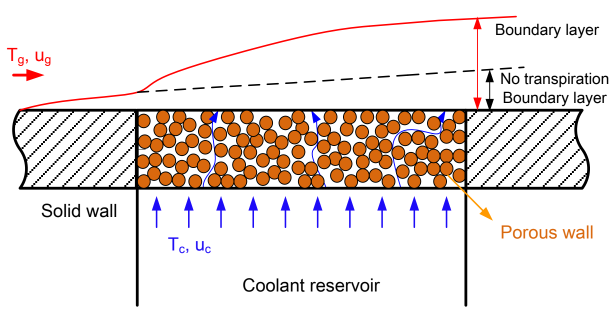

Figure 1: Computational domain

In this study, the main stream is coupled with a porous medium with local thermal non-equilibrium assumption. The flow inside the porous material is modelled using the Darcy–Brinkman–Forchheimer equation and the incompressible Navier-Stokes equations are solved for the main stream. At the interface between the main free stream and the porous zone, the couple conditions between the main flow temperature and the temperatures of the solid matrix and coolant flow within the porous media can be varied. And the calculated surface temperature can be extremely different when different conditions are assumed while it's vital important to predict the surface temperature accurately in case of thermal protection. Three kinds of condition are adopted as follows. Model A assumes the total heat flux was distributed according to the area ratio and the main flow temperature is calculated through the linear interpolation of the solid phase and fluid phase. Model B assumes main flow heat flux is the same with that imposed on the two phase of the porous medium. Model C assumes the main flow temperature equals the solid phase temperature and the main flow heat flux is all imposed on the solid phase. Numerical models with these three kinds of the couple conditions were analyzed.

NOMENCLATURE

F	=	Blowing ratio
h	=	Height of porous zone
H	=	Height of main flow zone
K	=	Permeability of porous media
l	=	Length of porous zone
L	=	Length of main flow zone
T	=	Temperature
V	=	Coolant inlet velocity
U	=	Main flow inlet velocity

Greek Symbols

ε	=	Porous media porosity

Subscripts

c	=	Coolant
m	=	Main flow
f	=	Fluid phase
s	=	Solid phase

1 Computational model

The physical model for the computations is shown in Fig. 2. The computational domain consists of a main flow zone and a porous zone. The height of the main flow zone is *H* and the length of the main zone is *L*. The porous plate is *l* long and the height is *h*. and h=0.5H, *l*=0.4*L*.The coolant flowed upward through the porous zone from the bottom with the same velocity V_c and an inlet bulk temperature T_c. The inlet main flow is fully developed with an average velocity U_m and the bulk temperature is T_f. The flow is laminar and incompressible. When the coolant inlet velocity V_c approaches zero, the flow tends to be Poiseuile flow.

A steady state analysis was used in the simulations. The steady governing equations for main flow written in their compact Cartesian form are:

$$\frac{\partial}{\partial x_{\mathrm{i}}}\left(\rho u_{\mathrm{i}}\right)=0 \tag{1}$$

$$\frac{\partial\left(\rho u_{\mathrm{i}} u_{\mathrm{j}}\right)}{\partial x_{\mathrm{i}}}=-\frac{\partial p}{\partial x_{\mathrm{i}}}+\frac{\partial \tau_{\mathrm{ij}}}{\partial x_{\mathrm{j}}} \tag{2}$$

$$\frac{\partial}{\partial x_{\mathrm{i}}}\left(u_{\mathrm{i}}(\rho E+P)\right)=\nabla\left(\lambda \frac{\partial T}{\partial x_{\mathrm{i}}}+u_{\mathrm{j}} \tau_{\mathrm{ij}}\right) \tag{3}$$

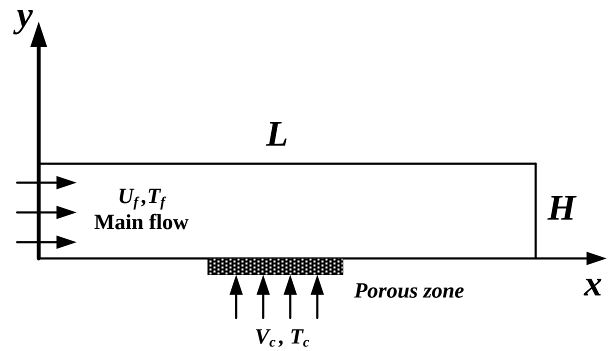

Figure 2: Computational domain

Where *E* is the total energy (= $h+u^2/2$ - p/ρ). The coolant flow through the porous media was modeled by the addition of a viscous term and an inertial loss term to the momentum equations based on the Brinkman-Forchheimer extended Darcy equation 4.

$$\begin{aligned}\frac{\partial\left(\rho \varepsilon u_{\mathrm{i}} u_{\mathrm{j}}\right)}{\partial x_{\mathrm{i}}}=&-\frac{\partial(\varepsilon P)}{\partial x}+\frac{\partial}{\partial x_{\mathrm{i}}}\left(\varepsilon \mu_{e} \frac{\partial u}{\partial x_{\mathrm{i}}}\right)\\ &+\frac{\varepsilon^{2} \mu_{\mathrm{f}}}{K} u-\frac{\varepsilon^{3} \rho F}{\sqrt{K}}|U| u\end{aligned} \tag{4}$$

Where ε is the porous media porosity, *K* is the permeability and *F* is the inertial factor. The local thermal non-equilibrium model (LTNE) is adopted to simulate the heat transfer within the porous media. The solid phase equation and fluid phase equation are shown as equation 5 and 6.

$$\nabla(\lambda_{s,eff} \nabla T_{s})=h_{v}\left(T_{f}-T_{s}\right) \tag{5}$$

$$\nabla(\rho c_{p} u T_{f})=\nabla(\lambda_{f,eff} \nabla T_{f})+h_{v}(T_{s}-T_{f}) \tag{6}$$

It should be noted that the coolant and main flow medium are the same and there is no species transportation. The physical property of the fluid is considered as constant for simplicity. And the relevant boundary conditions should be specified at the porous/fluid interface when the conjugate fluid flow and heat transfer problem is solved. The shear stress continuity model is adopted for the mass and momentum balance at the interface [6-7]. Nondimensional quantities are introduced for this problem.

$$Da=\frac{H^{2}}{K}; \quad \Lambda=\frac{F \varepsilon H}{\sqrt{K}}; \quad \mathrm{Re}_{f}=\frac{U_{m} H}{\upsilon_{f}}; \quad \mathrm{Re}_{c}=\frac{u_{c} H}{\upsilon_{c}}$$

$$U=\frac{u}{U_{\max}}; \quad Y=\frac{y}{H}; \quad \theta=\frac{T-T_{c}}{T_{f}-T_{c}}; \quad Bi_{c}=\frac{h_{v} h^{2}}{\lambda_{s,eff}}$$

Where U_{max} is the maximum velocity of the main flow. Because the physical property is treated as constants so the blowing ratio *F* can be obtained by $F=\rho u_c/\rho u_f=Re_c/Re_f$. Three different energy coupled models were analyzed. Model A assumes the total heat flux was distributed according to the area ratio and the main flow temperature is calculated through the linear interpolation of the solid phase and fluid phase [6-7].

$$T_f\big|_m = (\varepsilon T_f + (1-\varepsilon)T_s)\big|_{por}$$
$$-\lambda_f \frac{\partial T_f}{\partial n}\Big|_m = (-\lambda_{f,eff}\frac{\partial T_f}{\partial n} - \lambda_{s,eff}\frac{\partial T_s}{\partial n})\Big|_{por} \quad (7)$$

Model B assumes main flow heat flux is the same with that imposed on the two phase of the porous medium.

$$T_f\big|_m = (\varepsilon T_f + (1-\varepsilon)T_s)\big|_{por}$$
$$-\lambda_f \frac{\partial T_f}{\partial n}\Big|_m = -\lambda_{f,eff}\frac{\partial T_f}{\partial n}\Big|_{por} = -\lambda_{s,eff}\frac{\partial T_s}{\partial n}\Big|_{por} \quad (8)$$

Model C assumes the main flow temperature equals the solid phase temperature and the main flow heat flux is all imposed on the solid phase.

$$T_f\big|_m = T_s\big|_p$$
$$-\lambda_f \frac{\partial T_f}{\partial n}\Big|_m = -\lambda_{s,eff}\frac{\partial T_s}{\partial n}\Big|_p \quad (9)$$

2 Results and discussion

2.1 Fluid flow

The equations were numerically solved using finite element method. And the velocity distributions were shown in Fig. 3. Because the constant property was assumed in this work, the different energy coupled conditions had no effect on the effective viscosity which significantly changes the velocity profile.

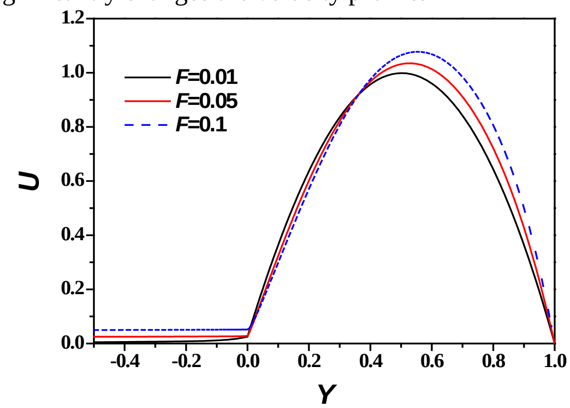

Figure 3: The horizontal velocity distribution for different blowing ratios (Re_f=100, Da=1e-3, ε=0.4, Λ=1.0)

The horizontal velocity distribution at the x=0.5H longitudinal section is shown in Fig. 3. The injection pushes the main flow fluid away from the porous/fluid interface and the velocity longitudinal distribution becomes more and more asymmetric with the increasing injection rate. As a result, the flow area for the main flow becomes small and the flow velocity away from the interface increases. The maximum velocity position moves towards the upper wall becomes larger than the inlet maximum velocity $U_{max.}$

2.2 Coupled boundary conditions

The energy equations of the LTNE model can be normalized by introducing following dimensionless parameters:

$$K = \frac{\lambda_{f,eff}}{\lambda_{s,eff}}; \quad X = \frac{x}{H}; \quad Pe = \frac{\rho c_p u H}{\lambda_{s,eff}}$$

$$\frac{\partial^2 \theta_s}{\partial X^2} + \frac{\partial^2 \theta_s}{\partial Y^2} = Bi_v(\theta_f - \theta_s) \quad (10)$$

$$Pe(\frac{\partial \theta_f}{\partial X} + \frac{\partial \theta_f}{\partial Y}) = K(\frac{\partial^2 \theta_f}{\partial X^2} + \frac{\partial^2 \theta_f}{\partial Y^2}) + Bi_v(\theta_s - \theta_f) \quad (11)$$

The Pe, K and Bi_v number have a significant effect on the temperature distribution reported by many researchers. When the difference between the solid and fluid conductivities increases, the LTNE effects emerge. The temperature difference between the fluid and solid phase decreases with the increasing Pe and Bi_v number, which means that the simulation results with the right coupled boundary conditions will approaches the LTE model results as the thermal non-equilibrium effect decreases. So it can be concluded that the right couple boundary conditions must obey that:

1. The solid phase temperature is larger than the fluid phase which promises that the transpiration cooling efficiency is less than 1.
2. The differences between the temperatures of the solid phase and fluid phase decreases with the increasing blowing ratio F and internal heat transfer coefficient h_v.

A. model A

The normalized fluid temperature and solid temperature are shown in Fig. 4. The flow conditions are kept the same (Re_f=100, Da=1e-3, ε=0.4, Λ=1.0, F=1%). And the ratio of the fluid and solid thermal conductivities K is 0.1 which is common when the porous media is made of sintered metal while the coolant is gas.

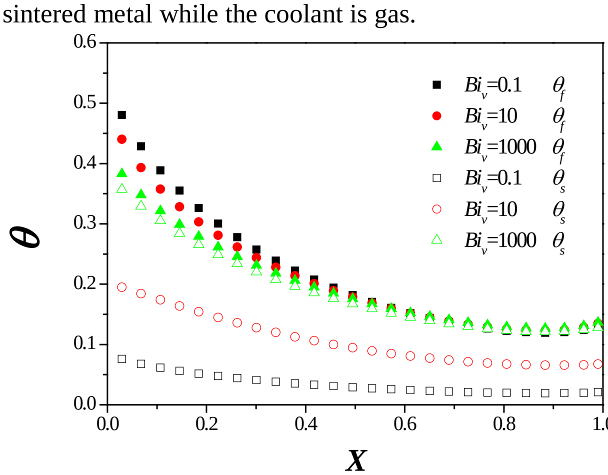

Figure 4: The temperature distribution on the porous-fluid interface

Figure 4 shows the temperature distribution of solid phase and fluid phase of porous media with different internal heat transfer coefficients. As the internal convective heat transfer enhances, the temperature difference between the two phases of the porous media decreases, and the thermal equilibrium can be assumed when the Bi_v approaches 1000. So the restriction 2 is satisfied according to the model A. However, the calculated fluid temperature is larger than the solid temperature along the main flow direction and the trend won't change with the increasing Bi_v. At the hot main stream side of the porous zone, the model A assumes the intrinsic heat flux of solid and fluid equals. When the thermal conductivity of solid is considerably larger than the fluid thermal conductivity, the temperature gradient of solid phase is dramatically small than that of the fluid phase for the moderate porosity. While the coolant side of the porous zone is set as the coolant inlet temperature, so the calculated surface solid temperature is small then fluid temperature. Generally, the result that the fluid temperature is larger is unphysical solution.

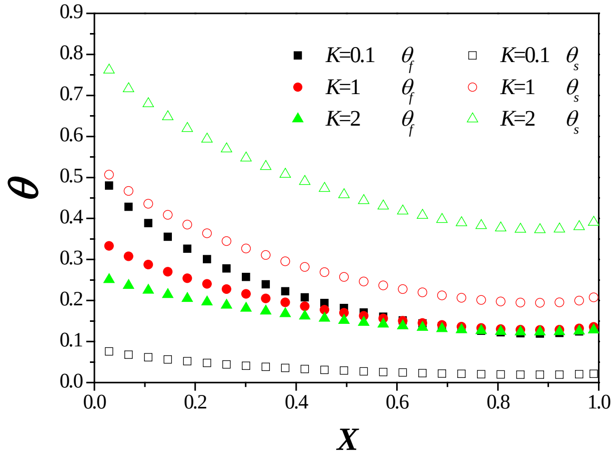

Figure 5: The temperature distribution on the porous-fluid interface for different thermal conductivity ratio K

Figure 5 shows that the calculated solid temperature will be higher than the fluid temperature only when the fluid thermal conductivity is equal or larger than the solid conductivity. And the results will be ridiculous except for these conditions. So the heat flux at the fluid and porous interface cannot be treated as distribution by the area ratio.

B. model B

Different from the model A which assumes the intrinsic averaged heat flux of the two phases equal, model B assumes each phase of the porous media receive the same imposed heat flux from the high temperature main stream. This kind of boundary condition is developed for the boundary conditions at the heated wall of the porous media with constant heat flux [8], and it is tested for the fluid/porous coupled circumstance here.

Figure 6 shows that the model B also gets illogical temperature distribution at the interface between the two calculation domains. Similarly, the temperature difference between the two phases decreases with the increasing *Biv*, and the calculated temperatures are higher than results in model A. So the calculation results give that the coupled model B will also descend that the interface fluid temperature is higher than the solid temperature. Thus, the boundary conditions in model A and B are not applicable for the coupled numerical simulation, especially when the difference between the thermal conductive of the solid and fluid phase is large.

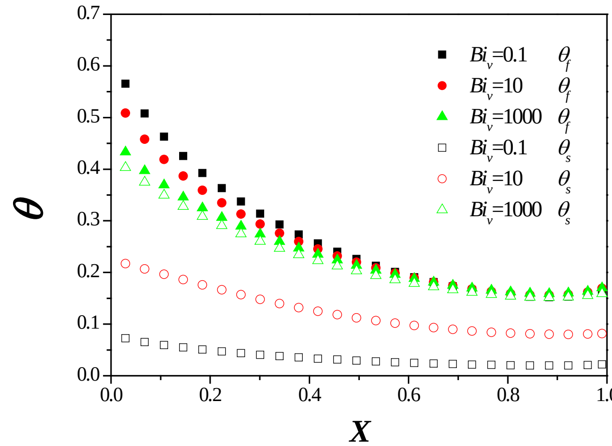

Figure 6: The temperature distribution on the porous-fluid interface for model B (K=0.1)

C. model C

Model C suppose the heat flux from the hot main stream is all conducted into the solid phase of the porous media, while the temperature of fluid phase equals with the main stream bottom side. When the heat flux from the main hot stream is all posted onto the solid phase of the porous media, the solid temperature is automatically larger than the fluid phase temperature within the porous zone. And the restriction 1 is satisfied. The internal temperature distribution is shown in Fig.7.

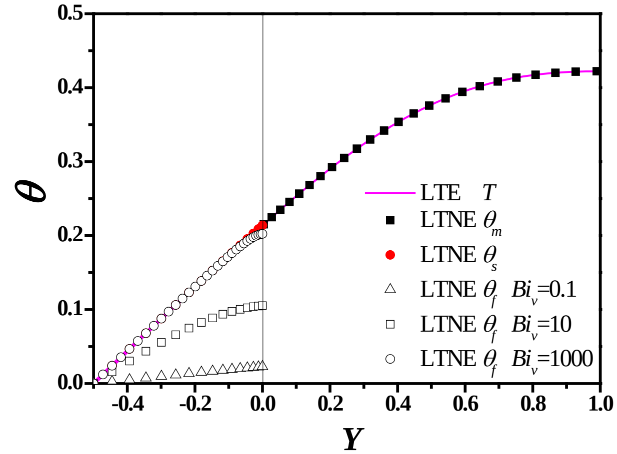

Figure 7: The temperature within the porous media for model C (K= 0.1, X= 0.5)

Figure 7 shows that model C sets the solid temperature equals with the main flow temperature at the fluid/porous interface for different internal heat transfer coefficients. Meanwhile, the coolant side boundary conditions for the solid phase keep at coolant inlet temperatures. Thus, the solid temperature distribution along the coolant flow direction keeps the same with the increasing *Biv*. The fluid temperature within the porous zone increases and LTNE effects diminishes as the increasing *Biv*, which satisfies the restriction 2.

CONCLUSIONS

In this study, the main stream is coupled with a porous medium with local thermal non-equilibrium assumption.

The flow inside the porous material is modelled using the Darcy–Brinkman–Forchheimer equation and the incompressible Navier-Stokes equations are solved for the main stream. The coupled boundary conditions at the interface between the main free stream and the porous zone are analyzed.

(1) Models assume that the heat flux from the main hot stream distributes as the area ratio of two phases of porous media will get unphysical solutions when the solid thermal conductivity is higher than that of fluid phase.

(2) Model C which assumes the main flow temperature equals the solid phase temperature and the main flow heat flux is all imposed on the solid phase can get reasonably right answer. And the simulation results can converge to the LTE results as the heat transfer within the porous media increases.

ACKNOWLEDGEMENT

The project was supported by a grant from the Foundation for Innovative Research Groups of the National Natural Science Foundation of China (No. 51321002) and the Industrial Technology Development Program (No. B1420110113).

REFERENCES

[1] Sreekanth and N. M. Reddy, Numerical Simulation of Transpiration Cooling Over Blunt Bodies at Hypersonic Mach Numbers, 30th AIAA Thermophysics Conference (1995).

[2] D. E. Glass, A. D. Dilley and H. N. Kelly, Numerical Analysis of Convection/Transpiration Cooling, Journal of Spacecraft and Rockets, 38 (2001) 15-20.

[3] Y. Q. Liu, P. X. Jiang, S. S. Jin and J. G. Sun, Transpiration Cooling of a Nose Cone by Various Foreign Gases, International Journal of Heat and Mass Transfer, 53 (2010) 5364-5372.

[4] F. Cheuret, J. Steelant, T. Langener, Numerical Investigations on Transpiration Cooling for Scramjet Applications Using Different Coolants, 17th AIAA International Space Planes and Hypersonic Systems and Technologies Conference (2011).

[5] J. H. Wang and H. N. Wang, A Discussion of Transpiration Cooling Problems through an Analytical Solution of Local Thermal Nonequilibrium Model, Journal of heat transfer, 128 (2006) 1093-1098.

[6] L. Betchen, A. G. Straatman and B. E. Thompson, A Nonequilibrium Finite-Volume Model for Conjugate Fluid/Porous/Solid Domains, Numerical Heat Transfer, Part A: Applications, 49 (2006) 543-565.

[7] H. J. Zhang, Z. P. Zou, Y. Li and J. Ye, Preconditioned Density-Based Algorithm for Conjugate Porous/Fluid/Solid Domains, Numerical Heat Transfer, Part A: Applications, 60 (2011) 129-153.

[8] X. L. Ouyang, K. Vafai and P. X. Jiang, Analysis of Thermally Developing Flow in Porous Media Under Local Thermal Non-Equilibrium Conditions, International Journal of Heat and Mass Transfer, 67 (2013) 768-77.